Semiconductors, 2025, Vol. 59, No. 5

Light-assisted gas identification using ZnO semiconductor sensors

© N.A. Klychkov, V.V. Simakov, I.V. Sinev

Saratov National Research State University,
410012 Saratov, Russia

E-mail: nklychkov@mail.ru

Received May 5, 2025
Revised August 9, 2025
Accepted August 9, 2025

This study investigates the photoresponsive and gassensing properties of zinc oxide (ZnO) thin films synthesized via the sol-gel method. A theoretical model is proposed to explain interband charge carrier generation under illumination and subsequent recombination through localized states induced by oxygen adsorption. Experiments reveal that UV irradiation significantly modulates the conductivity and dynamic response of ZnO-based sensors. These results demonstrate the potential of light-activated ZnO sensors for energy-efficient gas detection, with applications in environmental monitoring, industrial safety systems, and medical diagnostics.

Keywords: zinc oxide, sol-gel synthesis, thermal annealing, electrical conductivity, gas sensor, nanostructured materials.

DOI: 10.61011/SC.2025.05.61987.7910

Modern trends in gas sensorics are geared toward the production of next-generation semiconductor metal oxide sensors that are characterized by low energy consumption, increased safety of operation with flammable substances, and high durability [1]. Metal oxide gas sensors typically operate at elevated temperatures [2], which leads to uncontrolled thermal drift of their parameters and degradation of the gas-sensitive layer material and limits the applicability of sensors in detection of explosive gas mixtures [3]. In addition, semiconductor resistive gas sensors (chemoresistors) are sensitive to a wide range of gases and have low selectivity. Therefore, the issues of reducing the operating temperature of sensors and increasing their selectivity are the ones guiding the design of hardware components of gas sensorics.

Zinc oxide (ZnO) used as an active layer in gas sensors has attracted particular research attention due to a unique combination of electrophysical and chemical properties. Advances in nanotechnology have enabled the development of a wide range of gas-sensing zinc oxide nanostructures [4], which includes nanoparticles, nanowires, and complex three-dimensional structures. These ZnO nanostructures have a large specific surface area, which provides a significant improvement of their gas-sensing characteristics and allows them to operate at near-room temperatures [5,6]. It should be noted that zinc oxide is a wide-bandgap *n*-type material ($E_g \sim 3.2\,\text{eV}$), which is photosensitive in the region of intrinsic absorption ($\lambda < 400\,\text{nm}$). According to the data from [7], the absorption coefficient of zinc oxide at the indicated wavelength is $\gamma \approx 10^5\,\text{cm}^{-1}$.

This combination of material properties and the possibility of controlled synthesis of ZnO nanostructures of various morphology [8,9] open up broad prospects for the design of photoactivated gas-sensitive sensor systems. Such sensors have the capacity to operate at room temperature, providing an opportunity to control the conductivity level of their active layer via external optical influences [10,11].

The possibility of modulating the photoconductivity of ZnO nanorods by optical irradiation has been demonstrated in [12]. The role of oxygen recombination centers (O_2^-) has also been characterized there, but the mechanisms of influence of photostimulation on the gas-sensing properties of the material still remain understudied. The authors of [13] have demonstrated that UV irradiation enhances the adsorption of NO_2 on the ZnO surface due to the modification of electronic states; however, the used approach, which relies on Wolkenstein's theory, has been applied to oxidizing gases only. The authors of [14] have observed UV-stimulated switching of the response type of a ZnO sensor in detection of CO at temperatures below 100 °C, but a quantitative theoretical model has not been proposed. As far as we know, no quantitative models explaining the inversion of the response type of ZnO to reducing gases under illumination have been reported in literature to date.

Thus, the present study is aimed at developing a quantitative theoretical model characterizing the influence of optical radiation on the gas sensitivity of metal oxide gas sensors, which, in our view, is of academic and applied interest.

Active layers of ZnO-based gas sensors were synthesized via the sol-gel method with 1.25 g of zinc chloride ($ZnCl_2$) used as a precursor. This precursor was dissolved in 12 ml of ethanol at 80 °C and stirred for 30 min. The system had its pH adjusted to 5 (via the addition of an aqueous ammonia (NH_4OH) solution with a concentration of 25 %) and was held for 24 h at room temperature.

The formed gel was applied to alumina substrates cleaned with acetone by centrifugation (800 rpm), and the resulting layers were dried at 80 °C for 30 min. Further heat treatment of the deposited layers was carried out at 400 °C for 5 h in air. Chromium electrodes with an interelectrode gap

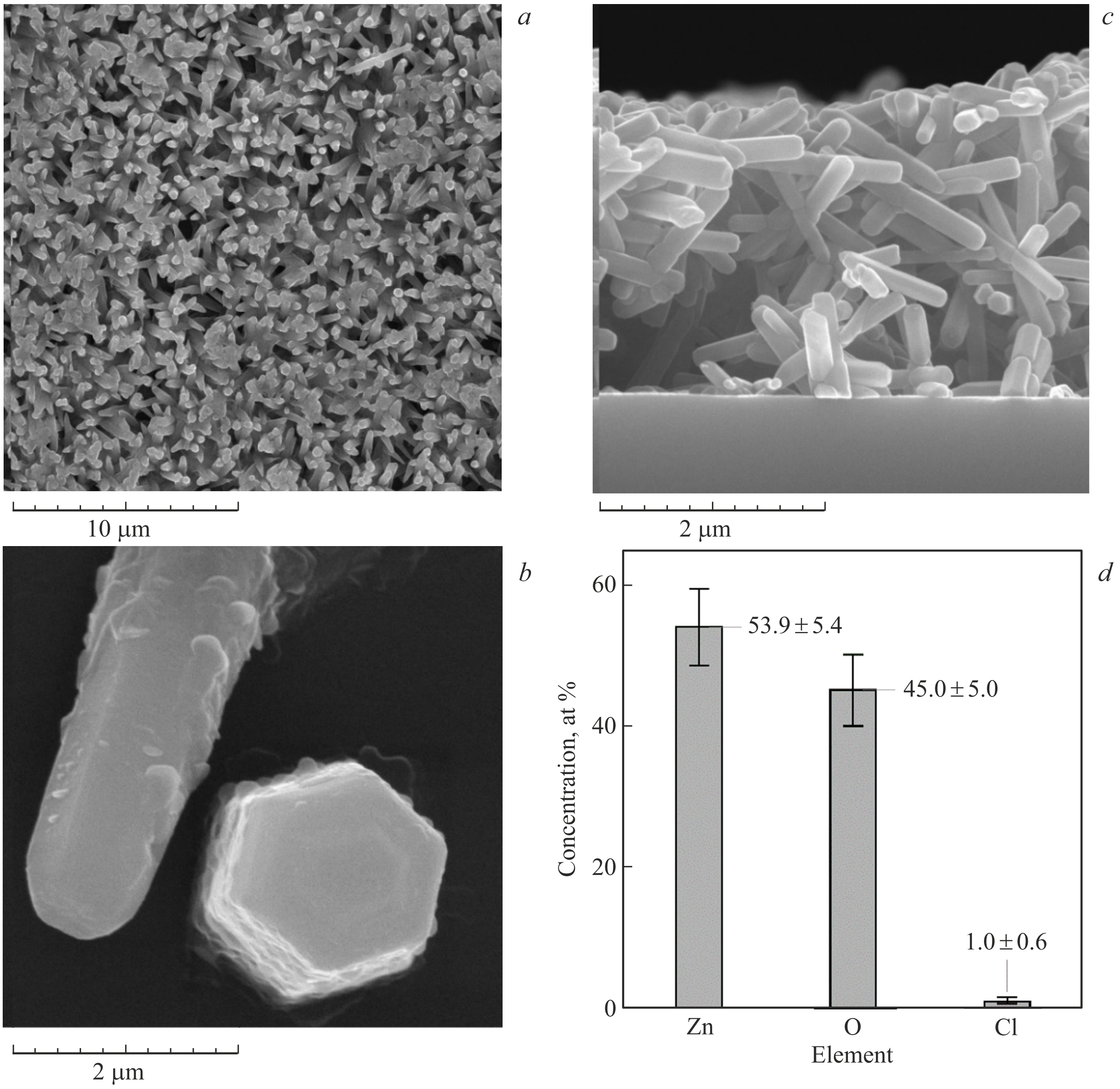

Figure 1. SEM images of the ZnO sample after annealing at 400 °C: *a* — surface morphology of the nanostructured layer; *b* — cleaved surface; *c* — individual hexagonal rod. *d* — Elemental composition of the material (errors are presented as confidence intervals).

of $40\,\mu$m for electrical measurements were applied to the annealed samples by thermal evaporation in vacuum.

Figure 1 presents the images of synthesized layers obtained by scanning electron microscopy (SEM) and the results of energy-dispersive spectral analysis.

Quantitative analysis of SEM images revealed that the synthesized gas-sensitive zinc oxide structures are an ensemble of hexagonal rod-shaped nanocrystals (Figure 1, *b*) with a characteristic lateral size of ~ 200 nm and a length of $\sim 1.2\,\mu$m. The thickness of the zinc oxide layer applied to the substrate was $\sim 2\,\mu$m. The concentration of chlorine in the ZnO layers determined experimentally via energy-dispersive spectral analysis (Figure 1, *d*) was 1.0 at.%, which is at the level of method error and insignificant.

The gas- and photosensitive characteristics of the obtained zinc oxide layers were examined at a temperature of 30 °C using a laboratory test setup [15]. The samples were illuminated by a UV LED (CHTPON, China) with a wavelength of 365 nm and a maximum power of ~ 3 W.

Experimental data obtained by exposing the samples to ethanol vapor (reducing gas) in the dark and at different illumination levels (I) are presented in Figure 2.

It can be seen from the figure that the conductivity increases reversibly under exposure to ethanol vapor in the dark. When the measurement chamber was purged with air, the conductivity of the studied ZnO samples fell to its initial value in air. This typical behavior of electrophysical parameters of the material is characteristic of a *n*-type semiconductor sensor exposed to reducing gases and corresponds to the so-called *N*-type response.

When the active layer of the sensor was illuminated with an intensity of $80\,\mathrm{mW\cdot cm^{-2}}$, the magnitude of ZnO conductivity change in the presence of ethanol decreased. A further increase in illumination intensity to $600\,\mathrm{mW\cdot cm^{-2}}$ led to inversion of the sensor response; i.e., the sensor conductivity decreased under exposure to ethanol. This is the *P*-type response: a reducing gas suppresses the conductivity of an *n*-type semiconductor.

A model of electronic processes based on the interband generation of carriers in ZnO with their subsequent recombination through deep surface levels induced by adsorbed particles of an oxidizing gas (e.g., oxygen) in the band gap of an *n*-type semiconductor was proposed as an explanation for the phenomena observed experimentally. It was assumed that the surface impurity levels of reducing gases are shallow donor levels and act as trapping centers for electrons. A system of equations was used to characterize the stationary nonequilibrium state of the system within the flat band model [16]. It included the conditions of adsorption-desorption equilibrium

$$P_a(N_s - N_a) = N_a^0, \qquad (1)$$

$$P_d(N_s - N_d) = N_d^0, \qquad (2)$$

the equations of carrier generation and recombination

$$c_n\left(n \cdot N_a^0 - n_a \cdot N_a^-\right) = \Phi, \qquad (3)$$

$$c_p\left(p \cdot N_a^- - p_a \cdot N_a^0\right) = \Phi, \qquad (4)$$

$$n \cdot N_d^+ - n_d \cdot N_d^0 = 0 \qquad (5)$$

and the equation of electroneutrality of the grain material

$$V \cdot \left(N_D^+ + p - n\right) = A \cdot \left(N_a^- - N_d^+\right), \qquad (6)$$

where $P_{a,d} = (\alpha P_0/\nu)\cdot\exp(W_{a,d}/kT_{\mathrm{gas}})$ is the normalized gas pressure; N_s, N_a, and N_d are the surface densities of adsorption centers and adsorbed particles of oxidizing and reducing gases, respectively; N^0 and N_a^-/N_d^+ are the densities of adsorbed particles in neutral and charged states; α is the Langmuir isotherm coefficient; P_0 is the partial gas pressure; ν is the characteristic phonon frequency; W is the desorption energy of particles of the corresponding type; $\Phi = \gamma F_0 d$ is the interband optical generation rate; γ is the absorption coefficient of the sample material; F_0 is the phonon flux; d is the characteristic grain size; c_n and c_p are the effective rates of carrier trapping at recombination centers; $n_a = N_c\exp(-E_a/kT)$, $p_a = N_v\exp\big((E_a - E_g)/kT\big)$, and $n_d = N_c\exp(-E_d/kT)$ are the concentrations of electrons in the conduction band and holes in the valence band when the quasi-Fermi level approaches the acceptor level of a recombination center E_a or the donor level of electron trapping E_d, respectively; N_D^+ is the concentration of shallow fully ionized donors in the bulk of a grain; and A and V are the surface area and the volume of a grain, respectively.

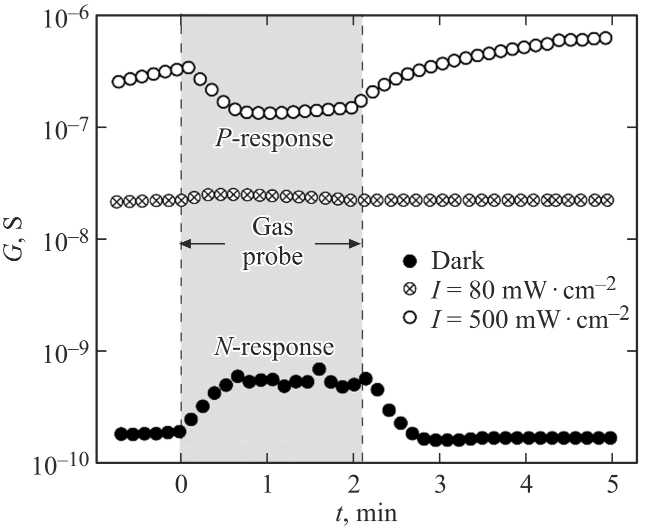

Figure 2. Temporal variation of conductivity (G) of the ZnO sample exposed to ethanol vapors with a concentration of 25 % of saturated vapor in the dark and at different illumination intensities (I).

To perform a comparative analysis of different types of response of the ZnO sample to reducing gases in the dark and under illumination, the gas sensor response was calculated as a relative change in conductivity of the active layer in gas:

$$S_N = (G - G_0)/G_0 \ \text{ by } \ G > G_0, \qquad (7)$$

$$S_p = (G - G_0)/G \ \text{ by } \ G < G_0, \qquad (8)$$

where G_0 and G are the sample conductivities in air and in gas, respectively. With the carrier mobility assumed to be constant, the latter quantity is defined as

$$G = q\,(\mu_n \cdot n + \mu_p \cdot p)\cdot\frac{S}{L}, \qquad (9)$$

where μ_n and μ_p are the carrier mobilities, S is the cross-sectional area of the sample, and L is the interelectrode distance.

System (1)–(6) was solved numerically with parameters characteristic of zinc oxide [17]. The results of calculations within the proposed model revealed that the magnitude and type of sensor response depend both on the intensity of optical excitation (Figure 3, *a*) and on the concentration of analyzed gas (Figure 3, *b*), which was confirmed experimentally (Figure 2).

Figure 3, *a* illustrates the effect of illumination intensity on the conductivity of the sensor structure in air and in a reducing gas. The conductivity in air increases with illumination intensity (primarily due to an increase in concentration of photoinduced holes). This is attributable to the fact that a significant fraction of photoinduced electrons are localized at the oxygen acceptor levels. At a certain threshold value of illumination intensity I_{inv}, the conductivity

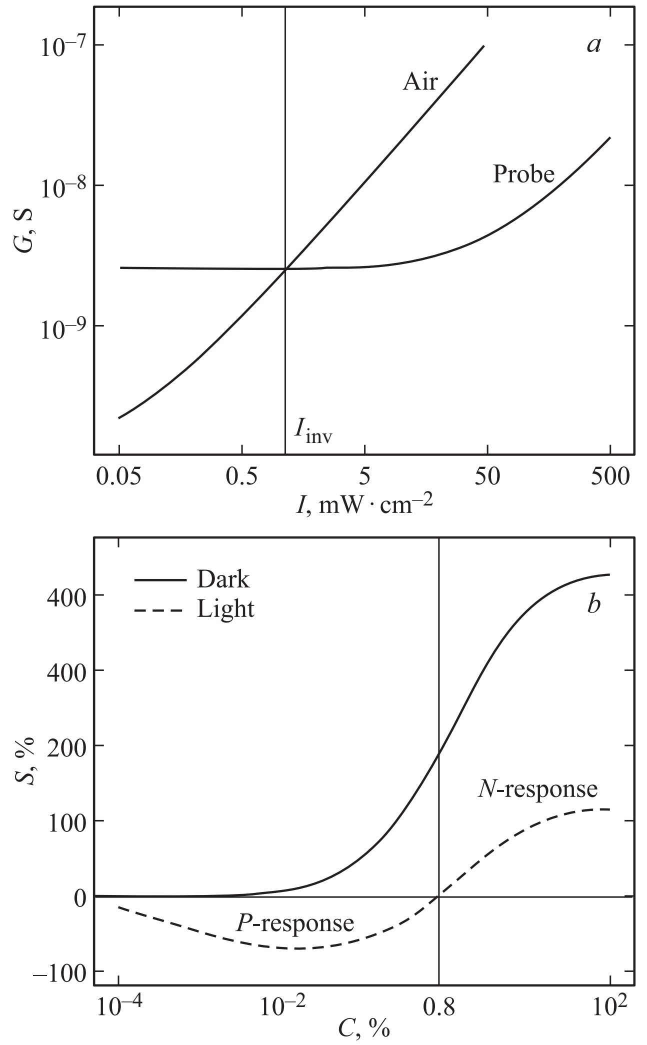

Figure 3. Calculated dependences of the sample conductivity in air and under the influence of a reducing gas with concentration $C = 0.05\,\%$ (a) and dependence of the sample response on the gas concentration in the dark and under illumination with $I = 10\,\mathrm{mW \cdot cm^{-2}}$ (b).

type of the semiconductor sample is inverted, and holes become the majority carriers in the material.

When a reducing gas is adsorbed, electrons are injected from the donor levels of this gas into the conduction band of the sample material, which leads to an increase in carrier recombination rate through the surface levels induced by adsorbed oxygen. The concentration of majority carriers (photoinduced holes) decreases as a result, and the conductivity of the sample as a whole decreases accordingly. This sensor behavior corresponds to a P-type response.

Figure 3, a demonstrates that the conductivity in a reducing gas exceeds the conductivity in air at illumination intensities below $\sim 2\,\mathrm{mW \cdot cm^{-2}}$, which is indicative of an N-type response. When the illumination intensity exceeds this threshold value, the response type gets inverted: the conductivity in analyzed gas becomes lower than the one in air, which corresponds to a P-type response. Thus, at a given reducing gas concentration, one may adjust the response type (N or P) of a gas sensor by modulating the intensity of illumination of its active layer.

Figure 3, b shows the dependence of the response type on the reducing gas concentration. The response is N-type at concentrations $> 0.8\,\%$, while lower concentrations correspond to a P-type response. This suggests the possibility of selective suppression of the sensor's response to certain analyzed gas concentrations via adjustment of the intensity of illumination of its active layer. This approach may be used to eliminate the influence of background impurities in multicomponent gas mixtures and odors.

Figure 4, a presents the experimental dynamics of response of the ZnO-based gas sensor to different reducing

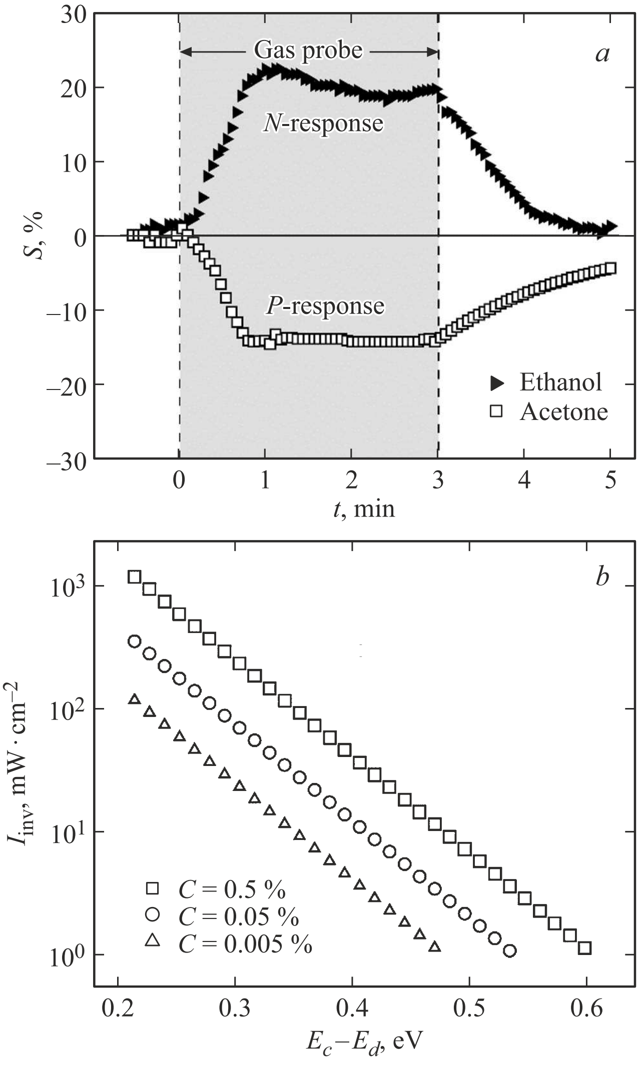

Figure 4. Dependence of the relative change in conductivity of the zinc oxide sample exposed to ethanol and acetone vapor: the vapor concentration is $50\,\%$ of saturated vapor, and illumination intensity $I = 30\,\mathrm{mW \cdot cm^{-2}}$ (a); theoretical dependence of the illumination intensity at which the response type changes (I_{inv}) on the position of the donor level of a reducing gas (b).

gases (ethanol and acetone) under a fixed illumination intensity ($I = 30\,\mathrm{mW} \cdot \mathrm{cm}^{-2}$). It can be seen that the responses of the gas sensor to the same concentrations of analyzed gases (ethanol, acetone) differ fundamentally.

At an illumination intensity of $30\,\mathrm{mW/cm}^2$, the response to ethanol does not get inverted, while a P-type response to acetone is observed under the same conditions.

The experimentally observed effect is apparently indicative of the influence of the energy position of donor levels induced by chemisorbed particles of reducing gases in the semiconductor band gap.

Figure 4, *b* shows the results of calculations focused on the influence of the depth of the donor level of a reducing gas on the illumination intensity corresponding to inversion of the sample response to the analyzed gas. It follows from the plot that the illumination intensity levels required for response type inversion (I_{inv}) differ in reducing gases that induce donor levels with different depths.

Thus, the variation of illumination intensity allows one not only to control the magnitude of a chemoresistive sensor's response to the analyzed gas, but also to obtain data on the depth of donor levels of various gases. This provides a potential opportunity to implement a spectroscopic approach to gas analysis: energy scanning of the band gap of the active layer material of chemoresistive gas sensors, which allows for an increase in selectivity and sensitivity in the analysis of multicomponent gas mixtures.

Photomodulation of conductivity of a semiconductor sample under illumination makes it possible to adjust the position of the Fermi level and induce an inversion of the sensor response type ($N{-}P$), providing a qualitative explanation for the experimental data presented in [18,19]. This opens up prospects for the development of new methods for identification of gases and the design of next-generation gas-analyzing systems with improved characteristics that operate at near-room temperatures.

A correlation between the results of calculations based on the proposed model and experimental data, which verify the possibility of controlling the gas-sensitive characteristics of ZnO-based gas sensors by illuminating their active layer material at a wavelength within the region of intrinsic absorption, was demonstrated. Under illumination, gas-sensitive ZnO samples exhibited an N-type response to ethanol vapors (their conductivity increased in gas) and a P-type response to acetone vapors (conductivity decreased in gas). This provides an opportunity to discriminate between gas media containing ethanol or acetone vapors not only by magnitude, but also by type of the gas sensor response.

Funding

This study was supported financially by the Russian Science Foundation (grant No. 24-29-00289).

Conflict of interest

The authors declare that they have no conflict of interest.

References

[1] V.V. Simakov, O.V. Yakusheva, A.S. Voroshilov, A.I. Grebennikov, V.V. Kisin. Techn. Phys. Lett., **32** (8), 725 (2006). DOI: 10.1134/S1063785006080256

[2] N. Yamazoe, G. Sakai, K. Shimanoe. Catalysis Surveys from Asia, **7**, 63 (2003). DOI: 10.1023/A:1023436725457

[3] G. Korotcenkov, B.K. Cho. Sensors Actuators B: Chem., **156** (2), 527 (2011). DOI: 10.1016/j.snb.2011.02.024

[4] Y. Wang, X. Li, N. Wang, Xie Quan, Yongying Chen. Separation and Purification Technol., **62** (3), 727 (2008). DOI: 10.1016/j.seppur.2008.03.035

[5] S.K. Gupta, A. Joshi, M. Kaur. J. Chem. Sci., **122**, 57 (2010). DOI: 10.1007/s12039-010-0006-y

[6] S.W. Fan, A.K. Srivastava, V.P. Dravid. Sensors Actuators B: Chem., **144** (1), 159 (2010). DOI: 10.1016/j.snb.2009.10.054

[7] H. Yoshikawa, S. Adachi. Jpn. J. Appl. Phys., **36** (10), 6237 (1997). DOI: 10.1143/JJAP.36.6237.

[8] N. Kirkwood, B. Singh, P. Mulvaney. Adv. Mater. Interfaces, **3** (22), 1600868 (2016). DOI: 10.1002/admi.201600868

[9] P. Tiwana, P. Docampo, M.B. Johnston, H.J. Snaith, L.M. Herz. ACS Nano, **5** (6), 5158 (2011). DOI: 10.1021/nn201243y

[10] I.V. Sinev, N.A. Klychkov, D.A. Timoshenko, V.V. Simakov. Fiz.-Khim. Aspekty Izuch. Klasterov, Nanostrukt. Nanomater., **12**, 713 (2020). (in Russian). DOI: 10.26456/pcascnn/2020.12.713

[11] M. Li, J. Chang, Z. Deng, L. Mi, M. Kumar, S. Wang, Y. He, G. Meng. Sensors Actuators B: Chem., **378**, 133115 (2023). DOI: 10.1016/j.snb.2022.133115

[12] A. Bera, D. Basak. Appl. Phys. Lett., **94**, 163119 (2009). DOI: 10.1063/1.3123167

[13] G. Li, Z. Sun, D. Zhang, Qi Xu, Leixin Meng, Yong Qin. ACS Sensors, **4** (6), 1577 (2019). DOI: 10.1021/acssensors.9b00259

[14] F. Bagheri, H. Haratizadeh, M. Ahmadi. Ceramics Int., **50** (1), 1497 (2024). DOI: 10.1016/j.ceramint.2023.10.240

[15] N.A. Klychkov, V.V. Simakov, I.V. Sinev, V.V. Efanova, A.M. Zakharevich. Fiz.-Khim. Aspekty Izuch. Klasterov, Nanostrukt. Nanomater., **16**, 891 (2024). (in Russian). DOI: 10.26456/pcascnn/2024.16.891

[16] V. Simakov, A. Voroshilov, A. Grebennikov, N. Kucherenko, O. Yakusheva, V. Kisin. Sensors Actuators B: Chem., **137** (2), 456 (2009). DOI: 10.1016/j.snb.2009.01.005

[17] N.A. Klychkov, V.V. Simakov, I.V. Sinev. Fiz.-Khim. Aspekty Izuch. Klasterov, Nanostrukt. Nanomater., **16**, 906 (2024). (in Russian). DOI: 10.26456/pcascnn/2024.16.906

[18] Y. Qin, X. Zhang, Y. Wang, Yi Liu. Sensors and Actuators B: Chem., **240**, 477 (2017). DOI: 10.1016/j.snb.2016.09.005

[19] Z. Dai, C.-S. Lee, Y. Tian, I.-D. Kim, J.-H. Lee. J. Mater. Chem. A, **3** (7), 3372 (2015). DOI: 10.1039/C4TA05438E

Translated by D.Safin